ADVANCED MATERIALS
www.advmat.de

Electric Eel-Skin-Inspired Mechanically Durable and Super-Stretchable Nanogenerator for Deformable Power Source and Fully Autonomous Conformable Electronic-Skin Applications

*Ying-Chih Lai, Jianan Deng, Simiao Niu, Wenbo Peng, Changsheng Wu, Ruiyuan Liu, Zhen Wen, and Zhong Lin Wang**

Electronic modules that are able to deform as desired, such as flexible, foldable, and even stretchable electronics, are considered as the next-generation electronics in the near future.[1–8] Such kinds of deformable electronics can provide the maximum freedom in the use of electronics, and thus can greatly broaden the applications of smart devices and sensor systems. For example, stretchable electronics can conformally apply on irregular, soft, or movable objects and organs, showing great potential in various fields ranging from wearable electronics to biomedical/implantable systems.[1–3,9] Although lots of research efforts on deformable electronics have been successfully demonstrated in various electronic components,[1–4,6–9] reliable and sustainable power sources still remain as one of the most crucial issues.[2,9–12]

Recently, triboelectric nanogenerators (TENGs), which can generate electricity by triboelectrification and electrostatic induction, have been demonstrated their capabilities to convert ubiquitous mechanical energy into electricity.[13–17] Especially, they show important uses in collecting low-frequency and irregular mechanical energy.[18–21] In order to scavenge the ambient energy in various dynamic and static mechanical conditions, it is highly demanded to develop mechanically durable and flexible TENGs. A flexible and stretchable TENG has been reported by assembling serpentine-patterned electrodes and a wavy-structured Kapton film.[21] However, the rigid materials used fairly restrict its stretchability, and it cannot apply in multiple and complicated mechanical deformations, hindering the TENG in wearable and conformal uses. Besides, due to the Young's modulus mismatch, the unstable adhesion between the rigid metal and elastic polymer is a fatal drawback to the reliability. Thus, to explore inherently mechanically durable TENGs is urgently essential.

Imitation and inspiration from nature are many today's innovations.[10,22–28] For example, human skin can be stretchable, body/shape conformal, and sense environmental stimuli like touch, pressure, and temperature. Electronics mimicking human skin, i.e., electronic skin (e-skin), have shown many potential applications, such as prosthetic/robotic skins, health monitoring, and human-interactive interfaces.[2,3,9,10,22,25] The capabilities of animal and insect skins also inspire more functions to such devices. For example, mimicking the function of chameleons' skin can be utilized to distinguish the applied pressure directly by capturing the change in device colors.[28] Inspired by cephalopod skin, optoelectronic systems can help adaptive camouflage in military applications.[27] Recent, a highly flexible electroluminescent skin has been reported.[22] Electric eel skin has a combination of soft feature and the capability to produce electricity while being attacked or irritated from surroundings (**Figure 1**a). Devices mimicking the capability of electric eel skin are expected to not only possess skin-like properties and body-conformability but also play as self-powered interactive interfaces. Competing to resistive or capacitive tactile sensors suffer from the need of rigid power sources.[2,10,28] Scientists also mimicked electric eels to develop flexible fiber-based capacitors with high output voltages.[26]

Softness, body/shape compliance and the capability of producing electricity are salient and special features of electric eel skins. To pursue those attributes, we present the first intrinsically mechanically durable and resilient nanogenerator by using triboelectric effects; skin-like triboelectric nanogenerator (SLTENG). The SLTENG realized through composed of intrinsic stretchable components can generate electricity from touch regardless of various extreme deformation required from uses, such as extreme omnidirectional stretch of over 300% strain, and multiple twists and folds. With the perfect flexibility, the nanogenerator can be fully conformal on various nonplanar or irregular objects, including human bodies, spheres, and tubes, etc., to act as power sources for other components. Particularly, even experiencing severe tearing damages, the device can retain its function as an effective power source for a load. The studies of the performance dependence on the thickness of dielectric layer, temperature, and applied forces have been included. And, the mechanisms about the influence on the performance at various kinds of deformation have been suggested. The produced

Prof. Y.-C. Lai, J. Deng, Dr. S. Niu, W. Peng, C. Wu, R. Liu, Z. Wen, Prof. Z. L. Wang
School of Materials Science and Engineering
Georgia Institute of Technology
Atlanta, GA 30332, USA
E-mail: zhong.wang@mse.gatech.edu
Prof. Y.-C. Lai
Department of Materials Science and Engineering
National Chung Hsing University
Taichung 40227, Taiwan
Prof. Z. L. Wang
Beijing Institute of Nanoenergy and Nanosystems
Chinese Academy of Sciences
Beijing 100083, China

DOI: 10.1002/adma.201603527

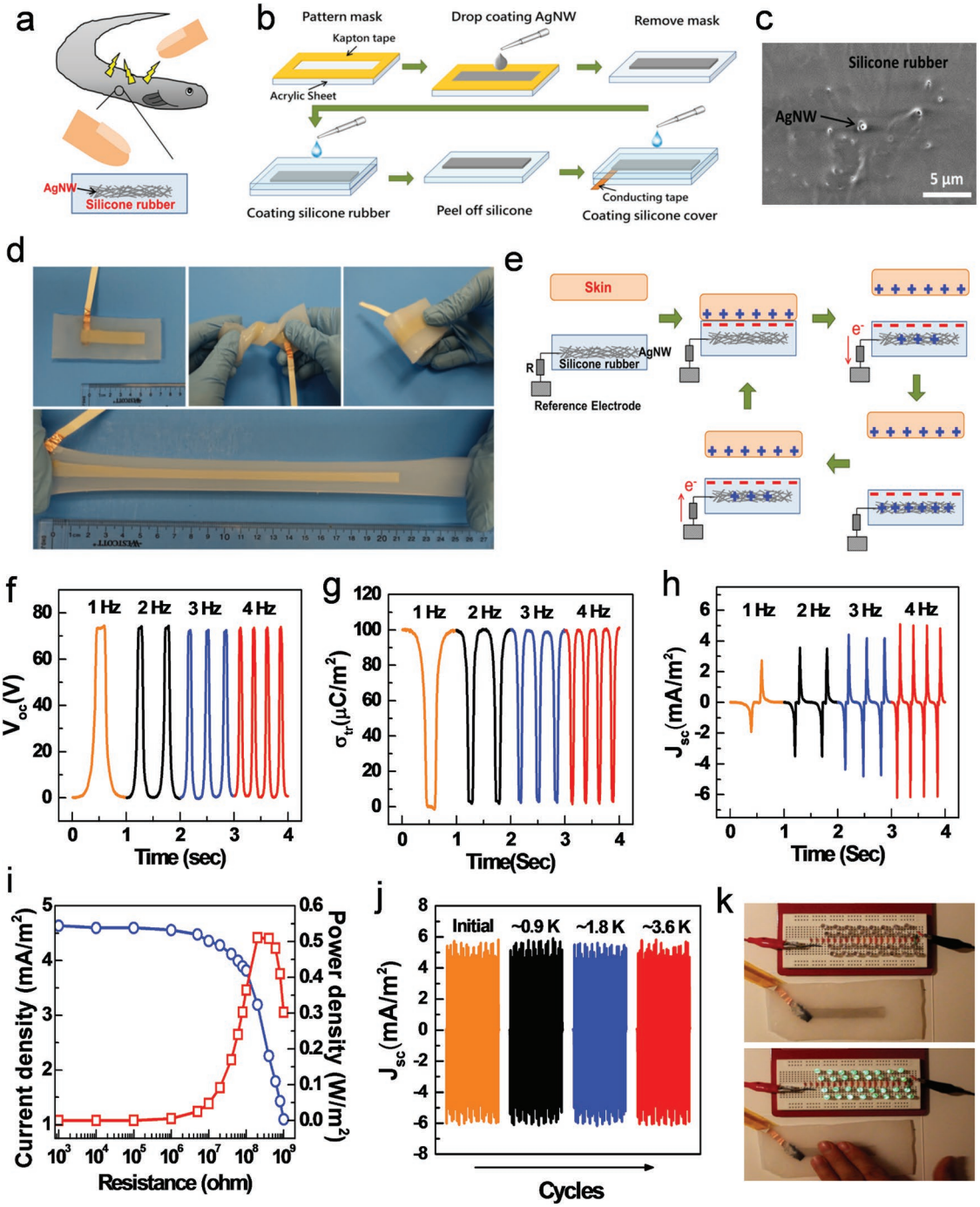

Figure 1. Electric eel's skin inspired nanogenerator. a) Illustration of the concept of an electric eel skin-inspired nanogenerator. b) Schematic diagram of fabrication processes. c) Side-view SEM image of as-prepared device. d) Photographs of as-prepared device with demonstrations of being different mechanical deformations including twist, fold and stretch. e) Schematic illustration of mechanism for generating electricity. f) V_{oc}, g) σ_{tr}, and h) J_{sc} of the nanogenerator. i) Relationship between instantaneous power density and resistance of the external load. j) J_{sc} after continuously operation for 900, 1800, and 3600 cycles. k) Photograph showing that 32 commercial green LEDs were lit up when the device was touched.

energy has been demonstrated to be able to sustainably drive a commercial smart watch. Based on the electric eel skin-like device, we further demonstrated the first fully self-sufficient and adaptive e-skin system that can map touch by responding with visual light-emitting diode (LED) signals without the need of external power supply. The presented results are timely and beneficial for the development of a wide range of deformable/wearable/biomedical electronics, self-powered human-interactive systems, and prosthetic and robotic skins.

Figure 1b depicts the schematic fabrication processes. Detailed fabrication methods can be found in the Supporting Information. Percolating silver nanowires (AgNWs) networks

Adv. Mater. 2016,
DOI: 10.1002/adma.201603527

were chosen as the conducting matrix owning to their superior merits of higher conductivity, flexibility, stretchability, low-cost, and easy-to-manufacturability.[29–34] Several reports have demonstrated that the interconnected 1D materials within percolating networks can effectively accommodate strain and exhibit higher stretchability than plastic materials such as organic conductors and buckled or serpentine metal thin films.[29–34] Another key material is the super-soft yet tough Eco-flex 00–10 silicone rubber that was chosen as the stretchable dielectric and encapsulated material of the SLTENG. Moreover, silicone rubber possesses a Young's modulus of below 1000 kPa which is much lower than skin.[35] It is also a very common material for designing prosthetic and prosthetic skin. And, the voids between the AgNWs enable silicone rubber to penetrate into the conducting network and embed the nanowires (Figure S1, Supporting Information). Figure 1c shows a cross-section scanning electron microscopy (SEM) image of the device, clearly showing the embedded AgNWs in the silicone rubber. It is worth to note that silicone rubber offers superior stretchability and resistance to tear propagation due to its high tear strength (Table S1, Supporting Information). Competing poly(dimethylsiloxane) (PDMS) that is the most commonly used as the elastic host in stretchable and flexible devices suffers from the low stretchability and lack of resistance to damage due to the low tear strength.[8] The devices are easy to shape and scale up as desired, and all of the processes are based on low (room)-temperature solution method, suggesting its advantages for cost-effective and industrial-friendly manufacturability. Figure S2 in the Supporting Information presents the skin-like nanogenerators with different sizes and shapes. Both components make the devices intrinsically stretchable and fairly durable to different extreme mechanical conditions. Figure 1d demonstrates a typical device in unstrained, twisted, folded, and stretched state.

The working mechanism of the SLTENG is schematically illustrated in Figure 1e, which involves a conjunction of contact triboelectrification and electrostatic induction.[14,15,36] Utilizing the different abilities to electron affinities, a transfer of surface charges occurs when skin touches silicone rubber. And, because silicone rubber has higher surface electron affinity than skin,[14,15,36] electrons would transfer from skin to the surface of rubber. The negative charges on the surface of rubber can induce positive charges in the mezzanine of AgNWs network as increasing the separation distance between skin and rubber, driving free electrons to flow from the AgNWs network to the reference electrode. This electrostatic induction process can give an output voltage/current signal to a load. When negative triboelectric charges on the silicone rubber are fully screened by the induced positive charges on the AgNWs network, no output signals can be observed. When skin approaches silicone rubber, the induced positive charges on the AgNWs network decrease, and the electrons flow from the reference electrode to the AgNWs network until skin and silicone rubber are fully contact each other again, resulting in a reversed output signal. This is a full cycle of the electricity generation process. A simulation result of the mechanism is presented in Figure S3 in the Supporting Information.

Typical output performances of the device including open-circuit voltage (V_{oc}), transferred charge density (σ_{tr}), and short-circuit current density (J_{sc}) were investigated by applying a 10 N contact force with different frequency, as shown in Figure 1f,g,h. The obtained V_{oc} approached over 70 V with a contact area of 2.5×2.5 cm^2. And, the amount of σ_{tr} can reach 100 μC m^{-2} (Figure 1g). This performance is much higher than previously reported structure-induced stretchable TENG (40 μC m^{-2} with two-layer electrodes)[21] and rubber-based TENG (9 μC m^{-2}).[37] The better results can be attributed to two reasons: (i) the higher difference of the surface electron affinity between silicone rubber and skin; (ii) the highly soft and conformal silicone rubber enabling the full contact between the skin and the surface of device, resulting in more efficient charge transfer. As a result, the J_{sc} reached to ≈6 mA m^{-2} at a contact frequency of 4 Hz. TENGs have demonstrated their superior capability in harvesting low-frequency energy, showing their promising applications in wearable and user-interactive uses.[18] Figure S4 in the Supporting Information shows the device performance depending on different contact forces. And, the device performances at different temperature have been studied in Figure S5 in the Supporting Information. The effect of thickness of silicone rubber was investigated in Figure S6 in the Supporting Information, indicative of the results that the thinner thicknesses of silicone rubbers reveal the better device performance. Moreover, the performance dependence on the number of times to deposit the AgNWs network was explored in Figure S7 in the Supporting Information, which indicates the fact that the more AgNWs in the network can provide the better device performance.

For different practical applications, the device can be used to drive loads with various resistances.[13–15] To evaluate its effective output power, the peak output current density and power density of the device were measured by externally connecting various resistance loads in series. The effective output power density was calculated as I^2R/A, where I is the output current across the external load, R is the load resistance, and A is the effective contact area. Figure 1i reveals the relationship between the output power density and the resistances. At the loading resistance below 100 MΩ, the J_{sc} reveals no significant decrease. The maximum output power density of 0.5 W m^{-2} could be achieved when the load resistance is about 200 MΩ. Figure 1j presents the measured results of the device after numerous operations, and the J_{sc} showed no significant degradation even after 3600 times operation. With such high performance, the SLTENG was able to instantaneously power up over tens LEDs in series by gentle touching (Figure 1k). It is also worth to compare the technology with other soft organic-based energy harvesters, such as piezoelectric and electrostrictive polymer (Table S2, Supporting Information),[38,39] the silicone-based TENG shows higher output and possesses a lower Young's modulus, which is more suitable for the uses that require high flexibility and stretchability, such as textiles and wearable/biomedical systems.

The device was tested for its capability of generating electricity in various extreme deformation conditions. First, it was evaluated at different tensile strain conditions in planar directions. As shown in **Figure 2**a left and Movie 1 in the Supporting Information, the device was manipulated under extremely stretching in the long-axis direction, and the device can perfectly harvest energy and drive a load. Figure 2a right shows

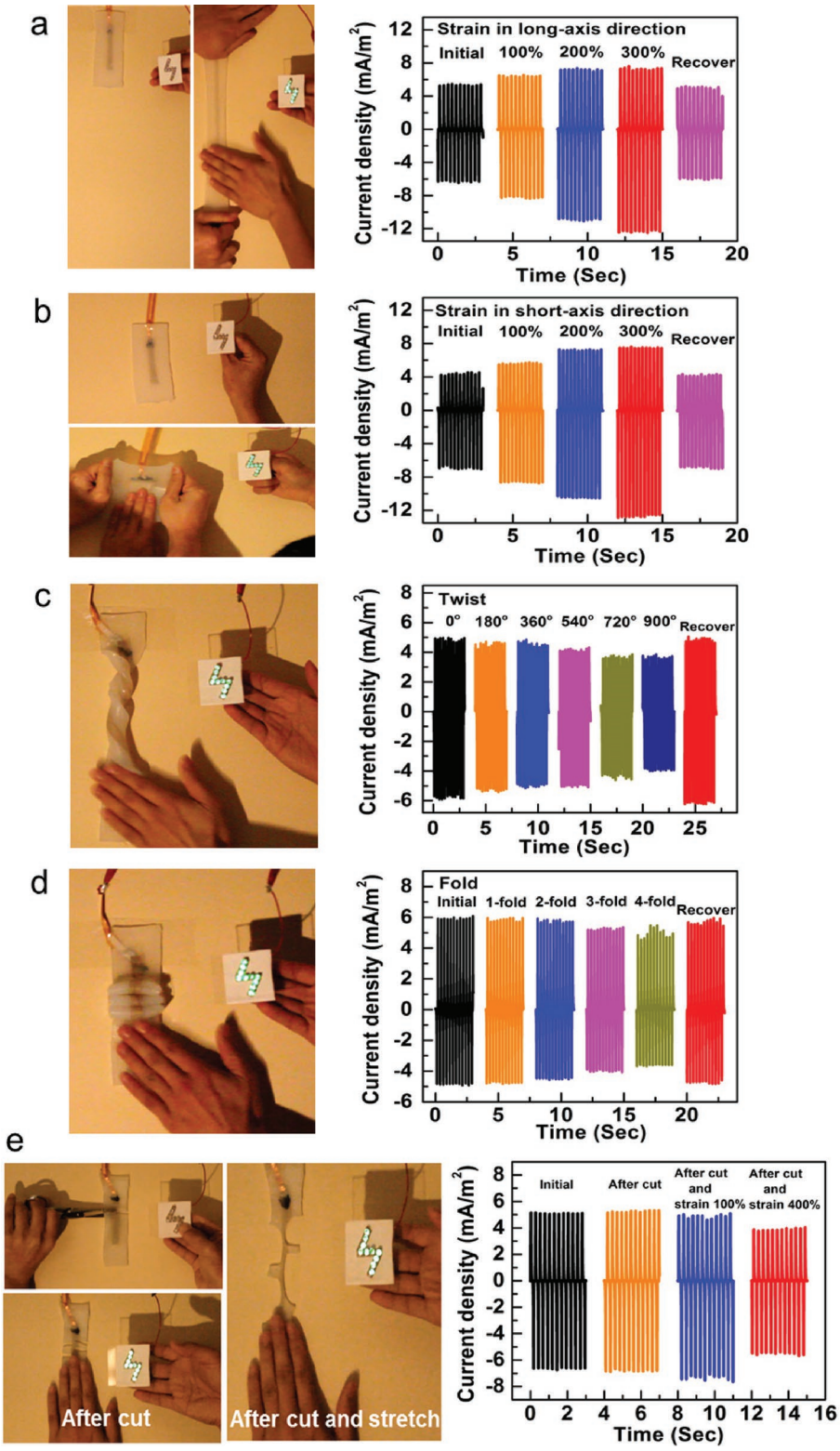

Figure 2. Evaluation of the nanogenerator under various deformations and even after being damaged. a) Left: Photograph demonstrating that the device can well function and drive a load when it was extremely stretched in long-axial direction. Right: J_{sc} at various strain levels in long-axial direction. b) Left: Photograph demonstrating that the device drove a load when it was extremely stretched in short-axial direction. Right: J_{sc} at various strain levels in short-axial direction. c) Left: Photograph demonstrating that the device drove a load when it was extremely twisted. Right: J_{sc} at different-level twists. d) Left: Photograph demonstrating that the device drove a load when it was multiply folded. Right: J_{sc} at different-times folds. e) Left: Photograph demonstrating that the device can drive a load and retain its stretchability even experiencing severe tear damages. Right: J_{sc} after being cut and stretched.

Adv. Mater. **2016**,
DOI: 10.1002/adma.201603527

the J_{sc} of the device at different tensile strain states in long-axis direction. Here, strain is defined as $(L - L_o)/L_o \times 100\%$, where L is the elongated length and L_o is the original length of the device. The J_{sc} increased with the strained length increasing. A more discussion about the influence of strain on device performance has been presented in a later paragraph. Even after extremely stretching to 300% strain, the device can recover to its original performance at unstrained state. We also tested the device stretched in short-axis direction (Figure 2b and Movie 2, Supporting Information). Similar to the results in long-axial strain, the J_{sc} increased as the short-axial tensile strain increased, and the performance can be retrieved when strain was released. Figure S8 in the Supporting Information shows the stress–strain curves of the silicone rubber and the composite device.

Beyond stretching forces, the SLTENG was tested by subjecting to severe torsional deformation. The size of the device for this test is 1 cm × 12 cm. Figure 2c left and Movie 3 in the Supporting Information demonstrate that the highly twisted device can power up a load. Figure 2c right shows the J_{sc} at different twisted levels, which reveals that the J_{sc} was slightly decreased when the device was continually twisted. This result can be ascribed to the increased resistance in the AgNWs network. However, the device can well retain its ability to produce electricity, and the J_{sc} remained high even when the device was extremely twisted to 900°. We also examined the device under multiple folds which represents extreme forms of mechanical bending. Figure 2d left and Movie 4 in the Supporting Information show that the device can maintain as a power source even after multiple folds, indicative of its excellent bendability. The J_{sc} of the folded device is presented in Figure 2d right. The result shows that the J_{sc} was slightly degraded as the folding times increased, which is similar to the influence in twisted deformation.

Furthermore, the superior tear strength of silicone rubber enables the device to retain functionality and stretchability even undergoing severe mechanical damages. The ability to generate electricity was investigated after four-time cutting the device in half through the conducting network. As shown in Figure 2e left and Movie 5 in the Supporting Information, the device can retain its functionality and power up a load even after experiencing several tearing damages. Moreover, due to the high tear strength of the silicone rubber, the device can keep its stretchability for over 300% tensile strain. The resulting J_{sc} are presented in Figure 2e right.

To further analyze the performance depending on the stretched status, we used a larger device with an area of 8×15 cm^2 to avoid Poisson's effect on the change of contact area and kept a contact force of 10 N. **Figure 3**a,b shows the V_{oc} and σ_{tr} under various strain levels. Figure 3c shows the statistic results. The performance of J_{sc} after repeatedly stretching at 150% strain is shown in Figure 3d, which shows that the J_{sc} can be remained in the same order of magnitude without obvious degradations even after stretching 1000 times. Besides, it is interesting to find that the device performances increased as the applied strain increased. The performance response to the deformation can be explained by the competing effects between the change in the thickness of dielectric layer and the change in the resistance of AgNWs network. When the strain level increased, the thickness of silicone rubber became thinner due to Poisson's effect, as illustrated in Figure 3e. As applying a stretching force in planar direction, the thickness of elastomer tended to compression, leading to the reduction of the distance between the surface charges on the surface of silicone rubber and the AgNWs network, resulting in the increase of output performance. These results are consistent with the performance dependence on the thickness of rubber (Figure S6, Supporting Information). Furthermore, a simulation result about the V_{oc} depending on the thinning thickness of dielectric layer after stretching is shown in Figure S9 in the Supporting Information. The result shows that when the surface charge density keeps as the same level, the V_{oc} increases as the thickness decreases, which is consistent with the trend of the experiment results. On the other hand, the device performance was degraded by the increased resistance of AgNWs network during deforming the device. The increased resistance can be explained by the fact that the electrical pathways in the network were fractured due to the change of the positions and orientations of nanowires after deformation.[30] And, the increased resistance resulted in a lower device performance. This effect can be indirectly validated by the results in Figure S7 in the Supporting Information, which clearly shows the fact that the conducting network with a higher resistance led to a lower performance. The effects of both the thinning dielectric layer and the increasing resistance of AgNWs network affected to the TENG performance simultaneously. Based on our results in Figures 3c and 2a,b, during stretching the TENG, the change in the thickness of silicone rubber had dominant effect, so increasing outputs were observed. And, to the deformation such as twist and fold, Poisson's effect in the thickness of silicone rubber was not significant, and the change in the resistance of AgNWs network caused the degradation in the device performance, as shown in Figure 2c,d.

Based on the ultrahigh stretchability and mechanical reliability of the SLTENG, we then designed larger area devices for more challenging tests including biaxially stretching and conformally wrapping on various nonplanar objects. **Figure 4**a and Movie 6 in the Supporting Information depict the device operated under biaxially stretching. The device area for this demonstration is 5×5 cm^2. As shown in Figure 4a and Movie 6 in the Supporting Information, energy can be generated even when the device was drastically stretched in biaxial directions. Furthermore, the unique merits of super-soft and toughness of the SLTENG render it fairly conformal on the surface of objects. Figure 4b and Movie 7 in the Supporting Information show the SLTENG with an area of 10×10 cm^2 fully wrapped and worked on a small sphere with a radius of 2 cm. In order to tightly encase the small sphere, the device was multiply stretched, twisted, and folded. Relied on its excellent mechanical properties, the highly deformed device still retained its capability to produce electricity and drive a load. The SLTENG can also conformally attach and function on a ball with large radius, as shown in Figure 4c and Movie 8 in the Supporting Information. It is also worth to note from Movie 8 in the Supporting Information that the device with such large area can produce electricity from anywhere finger touched on the device, indicative of the scalability of the processing methodology. For more challenging tests, the device was extremely stretched and wrapped on the

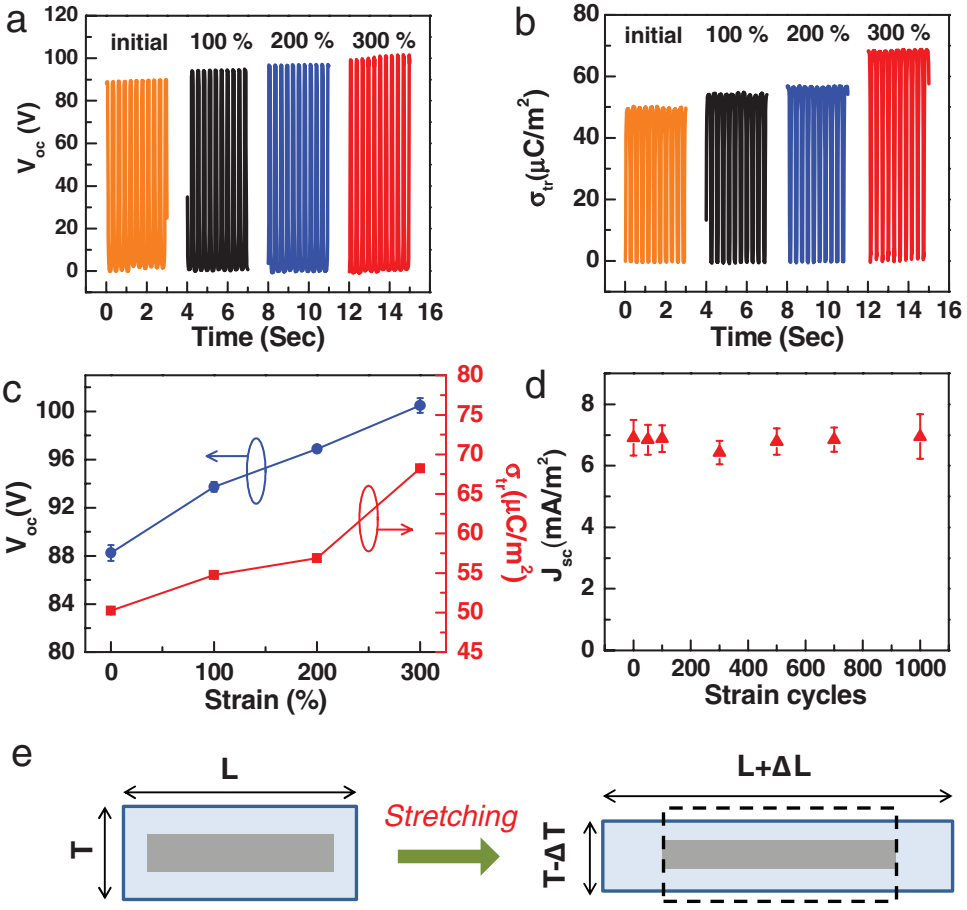

Figure 3. The measured results of a) V_{oc} and b) σ_{tr} after different strain levels. c) Statistic results of V_{oc} and σ_{tr} under various strains. d) J_{sc} after repeatedly stretching as 150% strain. e) Schematic illustration of Poisson's effect.

cap of the tube and showed no any rupture, clearly illustrating its toughness and softness (Figure 4d and Movie 9, Supporting Information). After that, the highly deformed SLTENG can maintain its capability. Above demonstrations show the capability of the SLTENGs to scavenge energy on various desired objects regardless of its physical presentation.

The generated energy can not only be directly used for driving loads but also be stored in a capacitor for later use. Figure S10 in the Supporting Information shows the charging result to a capacitor. And, with connecting to a power management circuit,[19] the harvested energy can be not only stored in the capacitor but also able to sustainably drive a commercial electronic systems simultaneously. Figure 4e and Movie 10 in the Supporting Information show the SLTENG was wrapped on a forearm, acting as a power wrister. Figure S11 in the Supporting Information shows the equivalent circuit for using as a sustainable power.[19] The charging voltage–time signal of the capacitor with connecting a power management circuit is shown in Figure 4f. Initially, both of the capacitor and the watch were out of electric energy. The collected energy was first stored in the capacitor. When the energy stored in the capacitor was sufficient to drive the watch, the voltage of the capacitor slightly dropped a little, and the watch started to work. As continuously tapping the device, the voltage of the capacitor would rise again, indicative of the fact that the harvested energy can not only drive the watch but also sufficiently charge the capacitor. This demonstration suggests that the device can use as a sustainable and body-adaptive power source for driving wearable gadgets, representing a fully self-powered electronic system.

Besides, utilizing the outstanding mechanical tolerance of the electric eel's skin-like device, a highly conformable and fully autonomous user-interactive e-skin system with visually human-readable signals was demonstrated. **Figure 5**a and Figure S12 in the Supporting Information show the prototype of the self-powered e-skin system, which presents a practical platform involving the integration of 3 × 3 SLTENG arrays and 3 × 3 LEDs matrix at a system level. Each SLTENG with an area of 1.5 × 1.5 cm^2 was directly connected with one LED in series. The unit of SLTENG serves as a power source as well as the touch sensing device. The electric eel's skin-like device allows us to realize a self-sufficient e-skin system without the need of data acquisition circuits and external power supply, which effectively circumvent the problems of battery and charging issue in the field of electronic skin.[2–4,25,28] This system can be utilized for instantaneous spatially mapping of touch with responding by visible LED signals. Figure 5b and movie 11 in Supporting Information present the e-skin system conformally contacted on an arm, acting as a self-powered artificial

Adv. Mater. **2016**,
DOI: 10.1002/adma.201603527

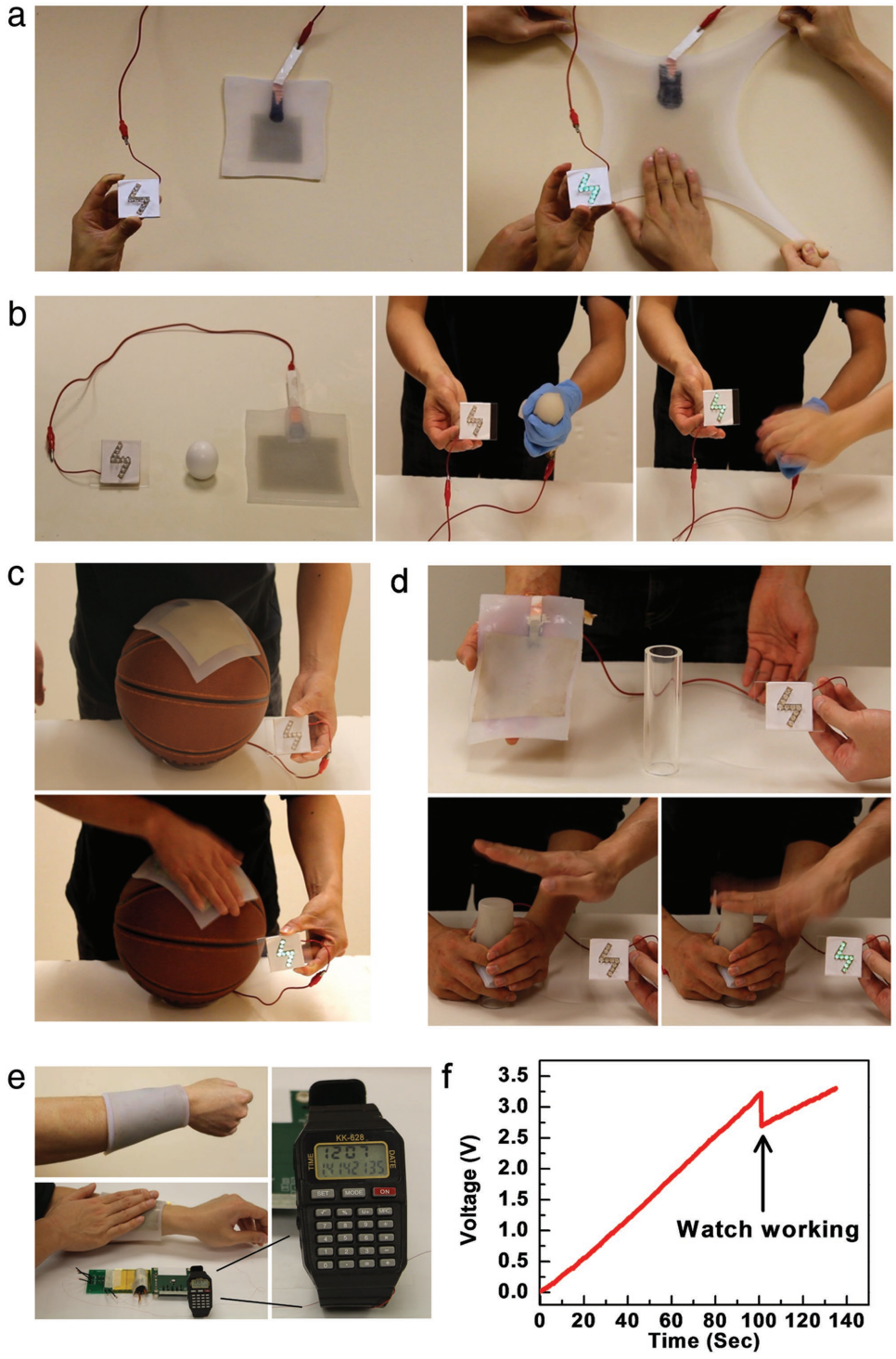

Figure 4. Demonstration of the generating function under biaxially stretching and on various nonplanar objects. a) Photograph demonstrating that the SLTENG drove a load when it was extremely biaxially stretched. b) Photograph demonstrating that the SLTENG drove a load when it fully wrapped a small sphere with a radius of 2 cm. c) Photograph demonstrating that the SLTENG drove a load when it conformally attached on a ball. d) Photograph demonstrating that the device drove a load when it wrapped the cap of a tube. e) Photograph demonstrating that the SLTENG worn on the forearm sustainably powered a commercial smart watch by hand tapping. f) Charging curve of the capacitor connected with a power management and smart watch by hand tapping.

mechanoreceptor. And, Figure 5c and Movie 12 in the Supporting Information show the system attached on a ball, acting as a force mapping system. The LED lit up intuitively corresponds to the unit touched by a finger. When a finger touches on the e-skin unit, the connected pixel of LED would be lit up in corresponding to the touching position. The presented

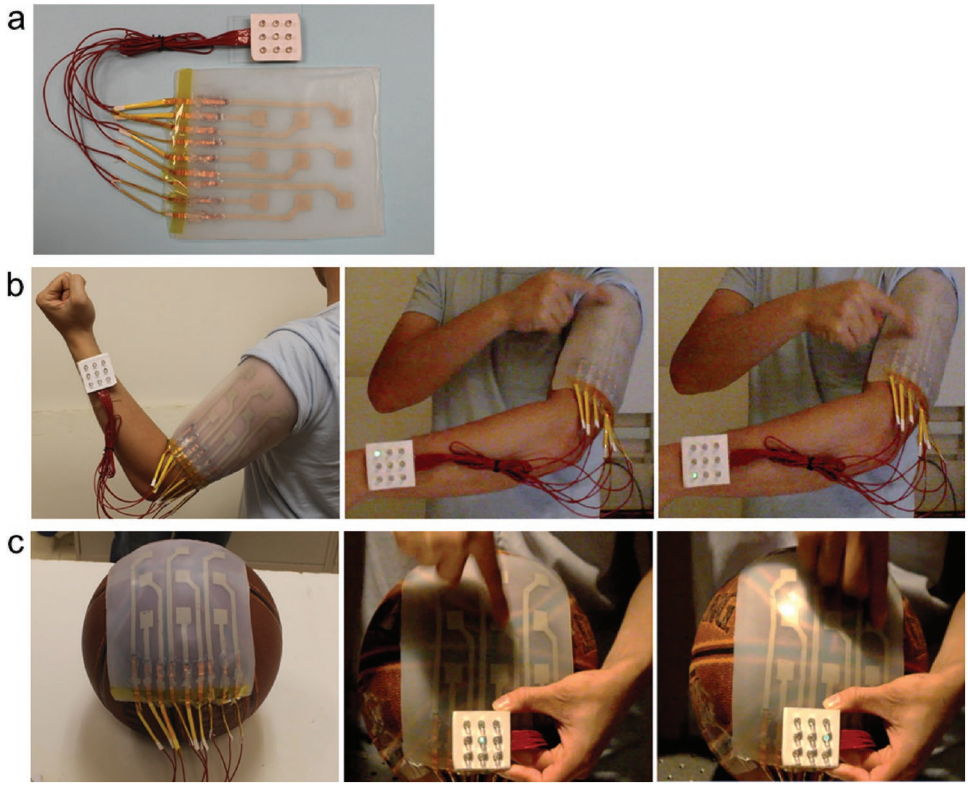

Figure 5. Demonstration of the fully autonomous and highly conformable e-skin system. a) Photograph of the fully autonomous and self-powered e-skin system. There is one-to-one relationship between the LEDs and the SLTENG units. b) Photograph demonstrating that the autonomously e-skin system conformally contacted on human arm and the LED lit up corresponded to the e-skin unit that being touched. Note that there is no external power supply in this system. c) Photograph demonstrating that the autonomously e-skin system conformally contacted on a ball and the LED lit up located to the unit that is being touched.

system is highly conformal and promising to long-term uses with self-supporting energy. In contrast to resistive- and capacitive-e-skin device,[10] our device shows an exceptional advantage that it does not need foreign power sources. It also shows the potential for directly integrating with other component for self-powered multifunctional e-skin uses.

In summary, a skin-like intrinsically mechanically durable and resilient triboelectric nanogenerator has been demonstrated the capability to produce electricity regardless of various extreme mechanical conditions and deformations. The device shows several breakthroughs in flexible nanogenerator devices, including biaxial stretchability, uniaxial stretchability of over 300% strain as well as the capabilities to multiple twists and folds and various desired deformations. Particularly, even experiencing severe tear damage, the device can well retain its functionality to generate electricity while maintaining its stretchability. These features can greatly broaden the nanogenerators to produce electric energy whenever desired. Based on the exceptional tolerability, the nanogenerator can be highly conformable on various nonplanar surfaces, promising immense applications in harvesting energy on arbitrary desired objects. With a large-area design, a reliable and wearable power source was demonstrated to sustainably drive a commercial watch. Utilizing the electric eel skin-like device, a fully self-sufficient and body-conformable e-skin system with intuitively visual signals was realized. The devices are easy to scale up and shape as desired, and the processes are cost-effective and suitable for industrial manufacture. These results are beneficial for a wide range of deformable electronics and autonomous interactive systems.

Supporting Information

Supporting Information is available from the Wiley Online Library or from the author.

Acknowledgements

This work was supported by the Hightower Chair Foundation and the "Thousands Talents" program for pioneer researcher and his innovation team, China. Y.C.L. thanks the funding support from Ministry of Science and Technology, Taiwan. Y.C.L. thanks Chao-Min Chen for her assistance in some experiments. J.D. would like to express his sincere gratitude to the China Scholarship Council (CSC) for the scholarship to help his study in the United States.

Received: July 4, 2016
Revised: August 15, 2016
Published online:

[1] S. I. Park, D. S. Brenner, G. Shin, C. D. Morgan, B. A. Copits, H. U. Chung, M. Y. Pullen, K. N. Noh, S. Davidson, S. J. Oh, *Nat. Biotechnol.* **2015**, *33*, 1280.
[2] M. L. Hammock, A. Chortos, B. C. K. Tee, J. B. H. Tok, Z. Bao, *Adv. Mater.* **2013**, *25*, 5997.
[3] B. C.-K. Tee, A. Chortos, A. Berndt, A. K. Nguyen, A. Tom, A. McGuire, Z. C. Lin, K. Tien, W.-G. Bae, H. Wang, *Science* **2015**, *350*, 313.
[4] T. Sekitani, H. Nakajima, H. Maeda, T. Fukushima, T. Aida, K. Hata, T. Someya, *Nat. Mater.* **2009**, *8*, 494.
[5] M. Drack, I. Graz, T. Sekitani, T. Someya, M. Kaltenbrunner, S. Bauer, *Adv. Mater.* **2015**, *27*, 34.
[6] D. J. Lipomi, Z. Bao, *Energy Environ. Sci.* **2011**, *4*, 3314.
[7] Y. C. Lai, Y. X. Wang, Y. C. Huang, T. Y. Lin, Y. P. Hsieh, Y. J. Yang, Y. F. Chen, *Adv. Funct. Mater.* **2014**, *24*, 1430.
[8] A. Chortos, G. I. Koleilat, R. Pfattner, D. Kong, P. Lin, R. Nur, T. Lei, H. Wang, N. Liu, Y. C. Lai, *Adv. Mater.* **2015**, *28*, 4441.
[9] S. Bauer, S. Bauer-Gogonea, I. Graz, M. Kaltenbrunner, C. Keplinger, R. Schwödiauer, *Adv. Mater.* **2014**, *26*, 149.
[10] A. Chortos, Z. Bao, *Mater. Today* **2014**, *17*, 321.
[11] M. Kaltenbrunner, G. Adam, E. D. Głowacki, M. Drack, R. Schwödiauer, L. Leonat, D. H. Apaydin, H. Groiss, M. C. Scharber, M. S. White, *Nat. Mater.* **2015**, *14*, 1032.
[12] S. Xu, Y. Zhang, J. Cho, J. Lee, X. Huang, L. Jia, J. A. Fan, Y. Su, J. Su, H. Zhang, *Nat. Commun.* **2013**, *4*, 1543.
[13] Y. Zi, S. Niu, J. Wang, Z. Wen, W. Tang, Z. L. Wang, *Nat. Commun.* **2015**, *6*, 8376.
[14] Z. L. Wang, *ACS Nano* **2013**, *7*, 9533.
[15] Z. L. Wang, J. Chen, L. Lin, *Energy Environ. Sci.* **2015**, *8*, 2250.
[16] R. Hinchet, S.-W. Kim, *ACS Nano* **2015**, *9*, 7742.
[17] M. Ha, J. Park, Y. Lee, H. Ko, *ACS Nano* **2015**, *9*, 3421.
[18] Y. Zi, H. Guo, Z. Wen, M.-H. Yeh, C. Hu, Z. L. Wang, *ACS Nano* **2016**, *10*, 4797.
[19] S. Niu, X. Wang, F. Yi, Y. S. Zhou, Z. L. Wang, *Nat. Commun.* **2015**, *6*, 8975.
[20] Q. Zheng, B. Shi, F. Fan, X. Wang, L. Yan, W. Yuan, S. Wang, H. Liu, Z. Li, Z. L. Wang, *Adv. Mater.* **2014**, *26*, 5851.
[21] P. K. Yang, L. Lin, F. Yi, X. Li, K. C. Pradel, Y. Zi, C. I. Wu, H. He Jr., Y. Zhang, Z. L. Wang, *Adv. Mater.* **2015**, *27*, 3817.
[22] C. Larson, B. Peele, S. Li, S. Robinson, M. Totaro, L. Beccai, B. Mazzolai, R. Shepherd, *Science* **2016**, *351*, 1071.
[23] J. Sambles, *Nat. Photon.* **2012**, *6*, 141.
[24] Y. M. Song, Y. Xie, V. Malyarchuk, J. Xiao, I. Jung, K.-J. Choi, Z. Liu, H. Park, C. Lu, R.-H. Kim, *Nature* **2013**, *497*, 95.
[25] C. Wang, D. Hwang, Z. Yu, K. Takei, J. Park, T. Chen, B. Ma, A. Javey, *Nat. Mater.* **2013**, *12*, 899.
[26] H. Sun, X. Fu, S. Xie, Y. Jiang, H. Peng, *Adv. Mater.* **2016**, *28*, 2070.
[27] C. Yu, Y. Li, X. Zhang, X. Huang, V. Malyarchuk, S. Wang, Y. Shi, L. Gao, Y. Su, Y. Zhang, *Proc. Natl. Acad. Sci. USA* **2014**, *111*, 12998.
[28] H.-H. Chou, A. Nguyen, A. Chortos, J. W. To, C. Lu, J. Mei, T. Kurosawa, W.-G. Bae, J. B.-H. Tok, Z. Bao, *Nat. Commun.* **2015**, *6*, 8011.
[29] F. Xu, Y. Zhu, *Adv. Mater.* **2012**, *24*, 5117.
[30] M. Amjadi, A. Pichitpajongkit, S. Lee, S. Ryu, I. Park, *ACS Nano* **2014**, *8*, 5154.
[31] C. Yan, J. Wang, X. Wang, W. Kang, M. Cui, C. Y. Foo, P. S. Lee, *Adv. Mater.* **2014**, *26*, 943.
[32] D. Langley, G. Giusti, C. Mayousse, C. Celle, D. Bellet, J.-P. Simonato, *Nanotechnology* **2013**, *24*, 452001.
[33] S. Lee, M. Amjadi, N. Pugno, I. Park, S. Ryu, *AIP Adv.* **2015**, *5*, 117233.
[34] Y. C. Lai, B. W. Ye, C. F. Lu, C. T. Chen, M. H. Jao, W. F. Su, W. Y. Hung, T. Y. Lin, Y. F. Chen, *Adv. Funct. Mater.* **2016**, *26*, 1286.
[35] D. Rus, M. T. Tolley, *Nature* **2015**, *521*, 467.
[36] Y. Yang, H. Zhang, J. Chen, Q. Jing, Y. S. Zhou, X. Wen, Z. L. Wang, *ACS Nano* **2013**, *7*, 7342.
[37] F. Yi, L. Lin, S. Niu, P. K. Yang, Z. Wang, J. Chen, Y. Zhou, Y. Zi, J. Wang, Q. Liao, *Adv. Funct. Mater.* **2015**, *25*, 3688.
[38] Y. Mao, P. Zhao, G. McConohy, H. Yang, Y. Tong, X. Wang, *Adv. Energy Mater.* **2014**, *4*, 130624.
[39] X. Yin, M. Lallart, P.-J. Cottinet, D. Guyomar, J.-F. Capsal, *Appl. Phys. Lett.* **2016**, *108*, 042901.